Isotope-selective trapping of doubly charged Yb ions

M. M. Schauer, J. R. Danielson, D. Feldbaum,* M. S. Rahaman, L.-B. Wang,† J. Zhang, X. Zhao, and J. R. Torgerson
Los Alamos National Laboratory, Los Alamos, New Mexico 87545, USA
(Received 7 October 2010; published 27 December 2010)

We report isotope-selective loading and trapping of doubly ionized ytterbium into an rf quadrupole trap. Isotopically pure clouds of $^{174}Yb^+$ ions were first loaded into the rf trap via a multistage photoionization process. The Yb^{2+} ions were then produced by electron impact ionization of the trapped Yb^+ ions. The Yb^{2+} ions were subsequently detected by rf excitation of their secular motion in the trap, which led to sympathetic heating and changes in the fluorescence of the laser-cooled Yb^+ ions. The presence of doubly charged Yb ions was further verified by the appearance of a dark band in the center of Yb^+ ion cloud after electron impact ionization. We discuss the possible formation of $Yb^{2+}H$ and similar compounds and the schemes for the direct optical detection of the Yb^{2+} ions.

DOI: 10.1103/PhysRevA.82.062518 PACS number(s): 32.10.−f, 37.10.Ty, 07.81.+a

I. INTRODUCTION

While singly charged ions have dominated the fields of atomic physics and quantum information because of the relative ease with which they can be produced and confined in rf traps, some multiply charged ions offer desirable characteristics that compel their study. For example, we proposed that doubly charged ytterbium (Yb^{2+}) could be used for a more sensitive test of time variation of the fine-structure constant when combined with measurements in singly ionized Yb^+ [1–3], and others have proposed to use it for fundamental studies in quantum optics as a near-ideal single-photon source [4]. Another relevant example is trapped Th^{3+}, which has been proposed as an ideal host to read out the state of the nucleus of ^{229}Th for its potential use as a nuclear clock of unprecedented stability [5,6]. Recently, $^{232}Th^{3+}$ was trapped and laser cooled [7]—the first time laser cooling was performed with a multiply charged ion.

As the ionization state increases, the valence electron generally becomes more strongly bound and transitions to the lowest energy states for laser cooling, and interrogation can move to higher energies, some outside the range of conventional laser sources. This is not universally true, and Yb^{2+} and Th^{3+} are notable counterexamples. Even so, highly frequency-stable laser sources now reach into the vacuum ultraviolet (VUV) [8–10], and synthesis of short wavelengths will improve over time, allowing future studies of previously inaccessible ions. In many cases, the level structure of multiply charged ions may not be well known, and it will be helpful to ascertain the presence of the ion in the trap through other means before the necessary laser wavelengths can be identified. We report such an alternative method here and demonstrate it by trapping and detecting sympathetically cooled, isotopically pure samples of Yb^{2+} ions.

II. ION TRAPPING

Linear rf traps achieve three-dimensional confinement by a combination of two different mechanisms. The ponderomotive force produced by an alternating electric quadrupole field confines ions in two dimensions, while a dc electric field prevents escape along the remaining degree of freedom. For our purposes, this arrangement can be thought of as a quadrupole mass filter with a dc potential applied to additional electrodes at the ends. A typical electrode configuration for producing the ponderomotive force is shown in Fig. 1. This provides confinement in the transverse plane. The resulting ion motion is governed by Mathieu's equation, the solutions of which yield ion oscillation frequencies given by

$$\omega_n = n\Omega \pm \omega_o, \tag{1}$$

where $n = 0,1,\ldots\infty$ [11]. We refer to motion of the ions at these frequencies as dipole since the motion can be driven with a dipole field at these frequencies. Vedel showed that quadrupolar excitation can also yield a response at $n\Omega - 2\omega_o$ [12], and we drive this motion as well in the following experimental work.

The fundamental ion oscillation frequency, or secular frequency, is

$$\omega_o \approx \frac{\Omega}{2}\sqrt{\frac{q^2}{2} + a}, \tag{2}$$

where $q = 4QV/m\Omega^2 r_o^2$ and $a = 2QU/m\Omega^2 r_o^2$. The quantities Q and m are the ion electric charge and mass, respectively; U and V are the dc and rf potentials applied to the trap rod electrodes, respectively; and r_0 is the characteristic transverse dimension of the trap.

Equation (2) is a good approximation for the secular frequency only if $a,q \ll 1$ [13,14]. As we shall see, for the experiments reported here $|a| \ll |q| \ll 1$, satisfying the preceding condition but additionally allowing Eq. (2) to be rewritten as

$$\omega_o \approx \left(\frac{q\Omega}{2\sqrt{2}}\right)\left(1 + \frac{a}{q^2}\right). \tag{3}$$

Substituting the values for a and q into this equation, we have

$$\omega_o \approx \left(\frac{q\Omega}{2\sqrt{2}}\right)\left(1 + \kappa\frac{U}{Q}\right), \tag{4}$$

where

$$\kappa \equiv \frac{mr_o^2\Omega^2}{4V^2}. \tag{5}$$

*Present address: Department of Physics, University of Florida, Gainesville, FL, 32611.
†Present address: Department of Physics, National Tsing Hua University, Hsinchu 30013, Taiwan.

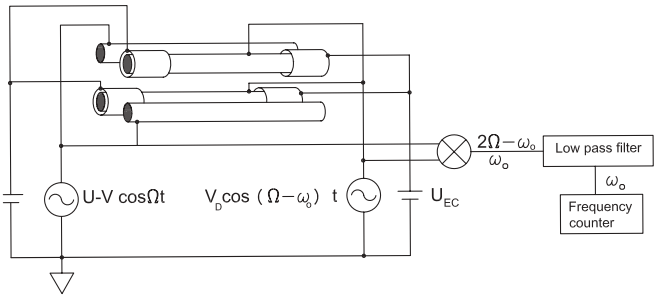

FIG. 1. Standard electrode configuration used in linear rf traps. An rf potential, V, and in some instances, a dc potential, U, are applied to two diagonally opposed rods, with the remaining two rods connected to ground. In these experiments, a low-amplitude drive signal, V_D, is applied to the ground rods to drive the motion of the ions in the trap, as described in subsequent sections of this article. Also shown in this figure are the endcap cylinders that provide axial confinement.

From the definition of q, it is obvious that the secular frequency of doubly charged ions for $U = 0$ is twice that of singly charged ions of the same mass. Equation (4) also shows that the secular frequency is shifted by a dc potential U applied to the trap electrodes and that the shift is proportional to Q^{-1}; that is, a doubly charged ion will experience half the shift experienced by a singly charged ion of the same mass.

Axial confinement is effected by means of additional endcap electrodes held at constant potential near the ends of the trap rod electrodes. The ions oscillate harmonically within this potential well in addition to the transverse motion described earlier. The axial motion is independent of the transverse motion caused by the ponderomotive force and generally occurs at a lower frequency. The presence of the additional axial potential also changes the secular frequencies of the ion motion in the transverse dimensions. To first order, the change to ω_0 is the same as applying the dc potential U to the rod electrodes, but with opposite sign and a different scaling factor that depends upon the endcap geometry. Equation (4) can thus be rewritten as

$$\omega_o \approx \left(\frac{q\Omega}{2\sqrt{2}}\right)\left(1 + \kappa\frac{U}{Q} - \kappa'\frac{U_{\rm ec}}{Q}\right), \qquad (6)$$

where $U_{\rm ec}$ is the endcap potential, and we determine κ' through numerical modeling of the trap geometry.

In the experiments reported here, the ponderomotive force is provided by an rf potential applied to 1 mm diameter, molybdenum rods with $r_o = 0.8$ mm. The frequency of the rf potential is 15.7 MHz, and the amplitude is roughly 600 V, yielding a secular frequency for Yb^+ of approximately 580 kHz. The axial well is produced by four endcap cylinders slipped over the ends of the grounded rods, as shown in Fig. 1. The separation of the inner edges of the cylinders is approximately 6 mm, and electrostatic modeling of the potential within the trap volume shows that the potential is harmonic to high degree over the central millimeter along the trap axis. Endcap potentials, $U_{\rm ec}$, of a few volts to as much as 165 V produce axial oscillation frequencies up to about 130 kHz. We operate with no dc potential applied directly to the trap rods but change the endcap potential $U_{\rm ec}$ to shift the secular frequency.

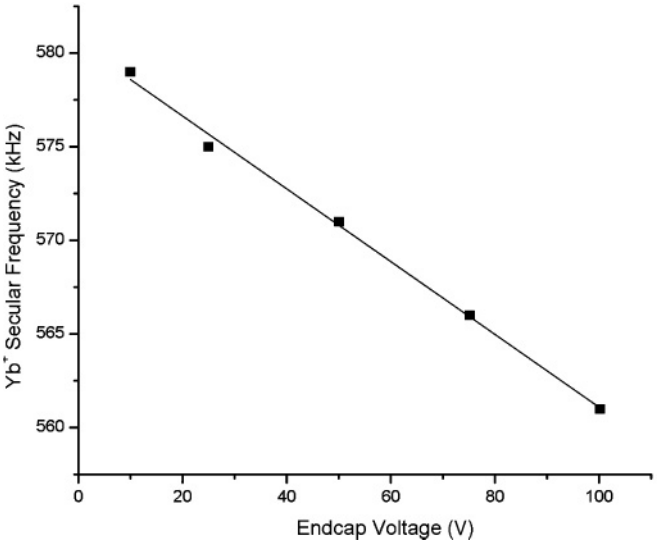

FIG. 2. Dependence of the secular frequency of singly charged Yb ions on endcap potential.

Figure 2 shows the measured secular frequency for $^{174}Yb^+$ as the endcap potential varies from 10 to 100 V. The data clearly show the expected linear dependence of the secular frequency on the applied dc potential. Fitting these data to Eq. (6) yields $q = 0.10$ and $\kappa' = 0.01$. The corresponding range of a parameters is roughly $-4 \times 10^{-4} < a < -4 \times 10^{-5}$ for 100 V $> U_{\rm ec} >$ 10 V. These results confirm that the condition $|a| \ll |q| \ll 1$ is satisfied in this apparatus.

III. ION LOADING

Ions are loaded into the trap by multiphoton ionization of neutral Yb atoms evolved from an oven consisting of a heated tantalum tube filled with Yb metal. The metal is not isotopically enriched but consists of the natural abundance of the Yb isotopes. Atoms are excited from the ^1S_o ground state to the $^1P_1$ state by light at 399 nm; it is this excitation which provides isotope selectivity in the loading process. From the $^1P_1$ excited state, the atom is ionized by absorption of either a 370 nm photon from the cooling beam (two-color photoionization) or another 399 photon (one-color photoionization) [15].

The atomic beam is collimated by a series of 1 mm diameter apertures and intersects the 399 nm photoionization beam at the center of the trap. This laser is locked to the absorption signal of a separate, external Ytterbium atomic beam source during the loading process. The collimation of the atomic beam and 90° intersection angle minimize the transverse Doppler width of the resonant step of the ionization process, thereby maximizing the isotope selectivity of the loading.

Although the work with doubly charged ions has thus far been limited to ^{174}Yb, we have routinely loaded pure samples of singly charged ions of all stable isotopes of Yb, with the exception of ^{168}Yb and ^{173}Yb. Table I shows the wavelength of the ground state to the $^1P_1$ excited state for those isotopes

TABLE I. Wavelength of the ^1S_o-$^1P_1$ transition in different Yb isotopes.

Isotope	Vacuum wavelength (nm)
^{170}Yb	398.9109(1)
^{171}Yb	398.9111(1)
^{172}Yb	398.9112(1)
^{174}Yb	398.9114(1)
^{176}Yb	398.9117(1)

we have trapped. It is interesting to note that the excitation wavelength we measured for ^{174}Yb with the corresponding frequency of 751.5264(2) THz is consistent with the recent measurement of 751.526 65(6) THz by Nizamani *et al.* [16], who noted a discrepancy with the previous result of 751.525987 761(60) THz by Das *et al.* [17]. Our wavelengths were measured with a Bristol 621 wavelength meter.

Doubly charged Yb ions are produced by electron impact ionization of the trapped singly charged ions. A low-current electron beam is produced by a tungsten filament located several millimeters from the trap electrodes and is accelerated to ≈100 eV before passing through the center of the trap where the Yb^+ are held. As charge exchange collisions are expected to be the dominant loss mechanism for the Yb^{2+}, the tungsten filament temperature is kept low enough that the system pressure does not exceed 1×10^{-10} torr during the ionization process. In this manner, we convert on the order of 25% of the singly charged ions to doubly charged ions after several minutes of electron beam bombardment. We then work with this mixed cloud of $^{174}Yb^+$ and $^{174}Yb^{2+}$.

IV. ION DETECTION

The singly charged ions are simultaneously detected and cooled by driving the $^2S_{1/2}$-$^2P_{1/2}$ transition at 370 nm. Light scattered from the 370 nm laser beam is imaged onto a photomultiplier tube and a camera, thereby allowing simultaneous photon counting and ion imaging. In addition to the 370 nm light, a repump beam at 935 nm is necessary

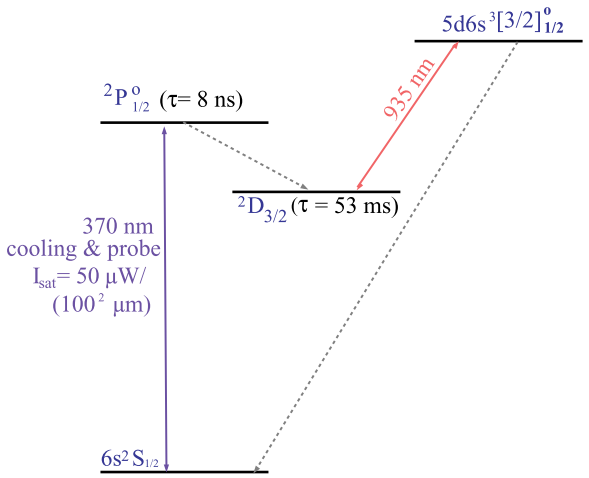

FIG. 3. (Color online) Relevant energy levels for optical detection of Yb^+.

TABLE II. Vacuum wavelengths of the cycling and repump transitions in selected isotopes of Yb^+.

Isotope	Cooling (nm)	Repump (nm)
$^{170}Yb^+$	369.5237	935.1978
$^{171}Yb^+$	369.5261 ($F = 1 - F' = 0$)	935.1880 ($F = 1 - F' = 0$)
$^{171}Yb^+$		935.1945 ($F = 1 - F' = 1$)
$^{172}Yb^+$	369.5245	935.1876
$^{174}Yb^+$	369.5250	935.1800
$^{176}Yb^+$	369.5256	935.1729

to return ions to the ground state from the $^2D_{3/2}$, to which an ion is expected to decay 1 in every 152 times through the $^2S_{1/2}$-$^2P_{1/2}$ transition [18]. Figure 3 shows the relevant levels, and Table II shows the results of our measurements of the vacuum wavelengths for these transitions for each of the isotopes we routinely trap.

Presence of the doubly charged ions was demonstrated through measurement of the frequency of the secular motion to establish the charge-to-mass ratio of the trapped ions. The secular frequency can be measured by applying a low-amplitude rf potential ($V_D \approx 0.1$ V) to two of the trap rods, as shown in Fig. 1, to drive the dipolar or quadrupolar motional resonances at $\Omega - \omega_o$ or $\Omega - 2\omega_o$. As the rf frequency is swept across the resonance, the kinetic energy of the ions increases, the cloud physically expands, and the Doppler broadening of the spectral line increases. Hence the spatial and frequency overlap of the ion cloud and the laser beam decreases significantly, leading to a dramatic reduction of the fluorescence from the cloud. Figure 4 shows a typical signal for singly charged Yb ions at their secular frequency ω_o. The same effect occurs when one drives the secular motion of nonfluorescing, trapped ions since the increased kinetic energy of the driven ions is rapidly redistributed to all ions in the trap through Coulomb collisions. Hence excitation of the secular motion of doubly charged Yb ions leads to an increase in the

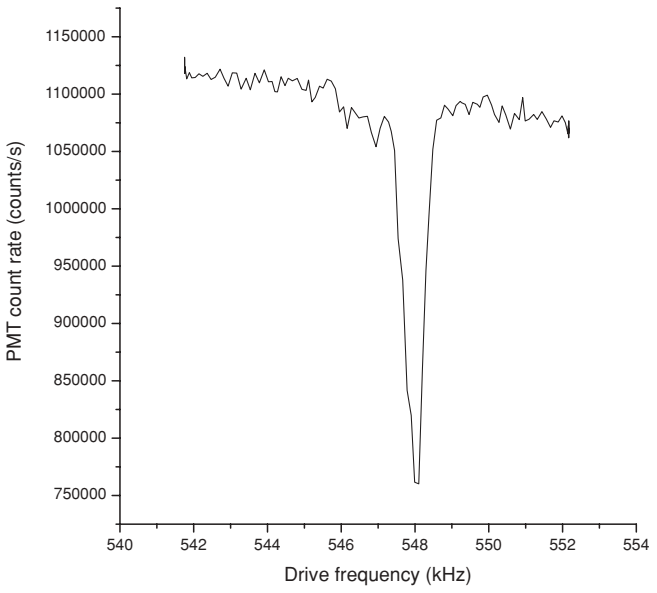

FIG. 4. Scan of Yb^+ secular frequency.

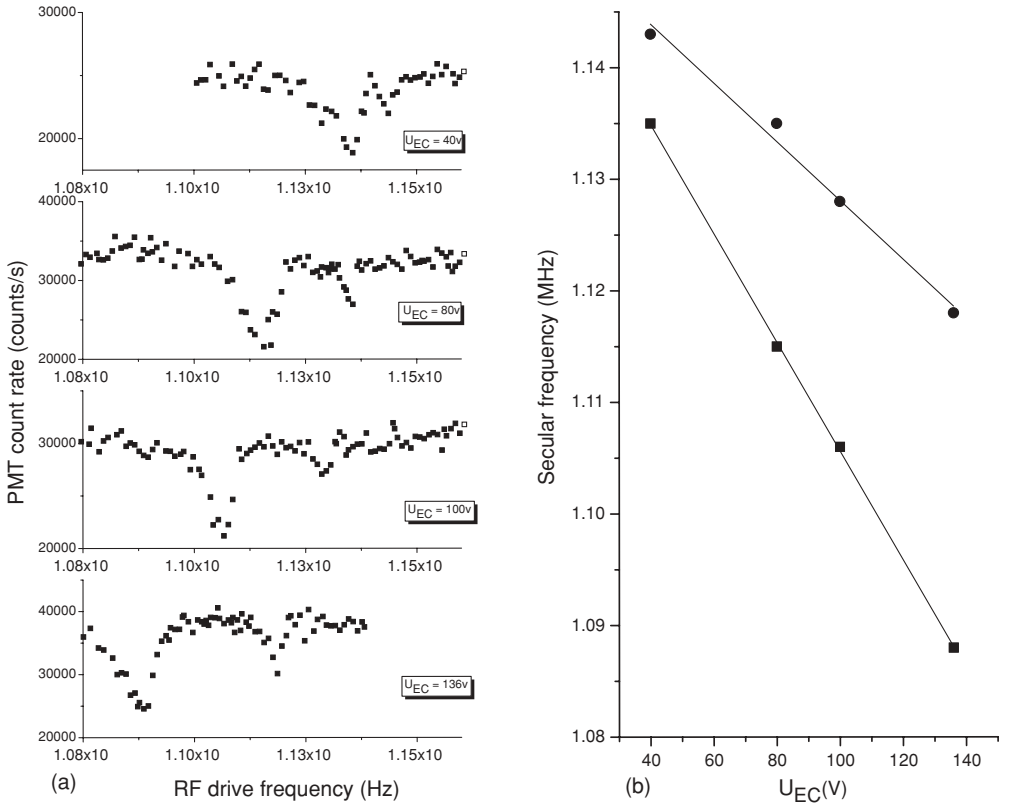

FIG. 5. (a) Results of sweeps of the secular frequency drive rf on mixed ion samples. (b) Linear fit results for the higher (circles) and lower (squares) frequency resonances are $\omega_{sec} = 1.1544(19) - 2.6(2)U_{ec}$ and $\omega_{sec} = 1.1544(5) - 4.88(6)U_{ec}$, respectively.

kinetic energy of the singly charged ions and a concomitant decrease in their fluorescence rate. Examples of this signal are shown in Fig. 5(a).

V. RESULTS AND DISCUSSION

As mentioned earlier, the unshifted secular frequency for Yb^{2+} is twice that of Yb^{+}, or about 1.1 MHz—close to the quadrupolar motional resonance of Yb^{+}. Therefore, in mixed clouds prepared in the manner described in the previous section, two resonances, nominally at twice the Yb^{+} frequency, are present with a small separation that is determined by the endcap potential. For $U_{ec} = 0$ and $U = 0$, the Yb^{+} dipolar and Yb^{2+} quadrupolar motional resonance frequencies are degenerate. Figure 5(a) shows the results of rf sweeps for such clouds for several different endcap potentials, while Fig. 5(b) shows a fit to the positions of the peaks as a function of endcap potential. The results are consistent with a factor of 2 difference in the slope, indicating that the lower frequency resonance is from Yb^{2+} ions.

A complicating effect is a slight shift of the secular frequency for clouds of ions much larger than those used for the work presented here. The secular frequency is lower for larger clouds ($N_{ions} \sim 10^6$) because of the decrease of the effective potential well in the trap caused by the space charge of the ion cloud [19]. To limit this effect, many of the measurements reported here were made with smaller clouds, and every reasonable effort to load the same size cloud for each measurement was made. Our primary diagnostic measurement for this purpose was the magnitude of the Yb^{+} fluorescence at 370 nm. We also accurately timed various stages of our loading and Yb^{2+} creation processes.

Furthermore, any ions not on the trap symmetry axis (the bulk of the ions in a large cloud) experience driven motion at the trap rf frequency, Ω, and this driven motion results in heating of the cloud. Obviously, both singly and doubly charged ions experience this driven motion, but only the $^{174}Yb^{+}$ ions are laser cooled, the doubly charged ions being cooled by Coulomb collisions with cold, singly charged ions. Hence the larger the total number of ions, and the larger the fraction of any given cloud that is doubly ionized, the higher the cloud temperature for a given laser power and detuning. The end result is that larger clouds, and those with a larger doubly charged component, are hotter so that the fluorescence signal at the photomultiplier is actually weaker than that of smaller clouds.

Mixed clouds of singly and doubly charged ions in our trap either were large, diffuse, and homogeneous or were smaller and brighter with sharp edges, often with a dark band at the center. Figure 6 shows a mixed cloud of the latter type. Generally, the diffuse, homogeneous clouds resulted when the electron beam was run for a longer time, presumably doubly ionizing a larger fraction of the cloud. Appearance of the dark band at the center of the ion cloud was accompanied by a rapid increase in the fluorescence signal as the cooling laser frequency was swept toward resonance from the low-frequency side. We attribute this behavior to segregation of the singly and doubly charged ions within the trap volume as

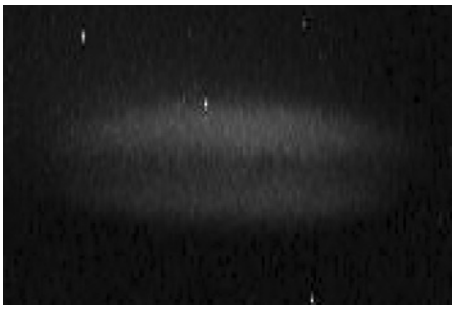

FIG. 6. A mixed cloud of singly and doubly charged ions. The dark band at the center of the cloud is consistent with segregation of the more tightly bound, doubly charged ions.

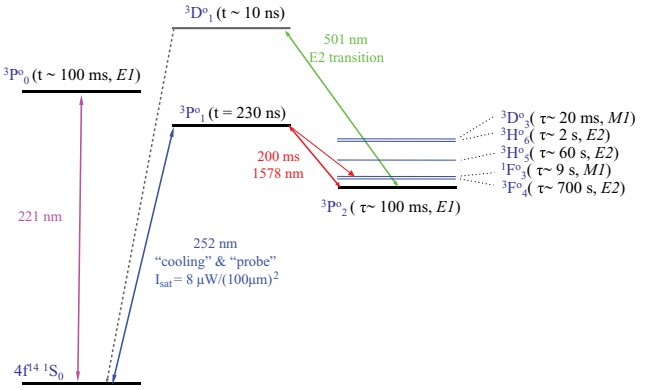

FIG. 7. (Color online) A partial energy-level diagram for Yb^{2+}. There exist several levels below the upper state of the cooling transition to which the ion can decay. Estimated lifetimes for the decay into and out of these levels is also shown. A Bates-Damgaard approximation was used to estimate the electric quadrupole transition rates.

the temperature of the ions is decreased. Since the effective well depth is a factor of 4 larger for the doubly charged ions than for the singly charged ones, the nonfluorescing, doubly charged ions preferentially occupy the center of the trap. Such behavior of multicomponent ion samples is well understood [20].

While developing the process for creating isotopically pure Yb^{2+} ions, we encountered several difficulties. We first attempted to create Yb^{2+} ions from trapped, isotopically pure Yb^+ ions by photoionizing them with 193 nm pulses from an ArF excimer laser. This method was ineffective since the poor quality of the excimer laser beam led to copious photoelectron and background gas emissions from the trap electrodes. Better results were attained with a tungsten filament operated at very low emission current: While the electron beam current through the trap was kept below 200 μA, the system pressure remained below 1×10^{-10} torr. This proved to be critical to the successful production and trapping of the doubly charged ions.

Initially, however, the base pressure of the system was limited to 4×10^{-10} torr by a small leak even in the absence of electron emission from the filament. With this pressure, trace amounts of N_2 and CO_2, as measured by a residual gas analyzer, limited our Yb^+ ion trap lifetime, as indicated by a decay in the ion fluorescence signal over several tens of minutes. Using the same method as that used to detect the presence of Yb^{2+} ions, we were able to determine that molecular ions, most likely $YbCO^+$ [21], were being formed. Illumination of the trapped ions by $\sim$100 μW of 252 nm light focused to $\approx$50 μm restored the full fluorescence signal, suggesting that the culprits were ionic complexes of Yb^+ and CO with a dissociation energy less than the 4.9 eV of the 252 nm photons. Upon locating and eliminating the leak, the vacuum system base pressure dropped to 4×10^{-11} torr, and our ion loss rate became immeasurably small ($^{174}Yb^+$ lifetimes $>$8 hours).

Although reactions between ground-state Yb^+ and hydrogen are energetically forbidden, reactions of excited Yb^{+*} with hydrogen are known to occur [21,22]. Hence the long lifetime of the singly charged ions would indicate a very low hydrogen density in our system. A quantitative estimate of this density is difficult to reach since the effective rate will, presumably, depend in some complicated fashion upon the relative powers of the 370 nm cooling and 935 nm repump laser beams. Despite the apparent paucity of hydrogen, we cannot rule out reactions between the doubly charged ions and neutral hydrogen: The fractional mass resolution of our detection system, $\Delta m/m$, is at best a few percent.

Obviously, the way to lay these doubts to rest is to detect the Yb^{2+} ions optically. This could be achieved by driving the ^1S_o-$^3P_1$ cooling transition at 252 nm [23], and we have constructed a frequency quadrupled source based on a 500 mW Ti:sapphire laser to synthesize light for this purpose. However, as can be seen from Fig. 7, the possibility of optical pumping into one of the six states between $^1S_0$ and $^3P_1$ exists, and repump light of some form may be necessary. For example, light at 1598 nm would couple the $^3P_2$ and $^3P_1$ states and repump any population in the $^3P_2$ state. Alternatively, an Yb plasma source could be used to depopulate the remaining states below the $^3P_1$ state with light directly from the discharge, a technique that has been demonstrated in trapped Ba^+ [24].[1]

VI. CONCLUSION

The loading and detection method of multiply charged ions described here is generally applicable to any ion. It allows detection of multiply charged ions whose electronic energy levels may not be well known, as long as an ion of lower charge state can be laser cooled and detected. Although we demonstrated the technique with doubly charged ions, it can certainly be applied to higher charge states: The only limitation is the ability to produce and store ions of the desired charge state in large enough quantities to be detectable and, possibly, limitations of the drive electronics as the secular frequency increases.

As described in the previous section, chemical reactions with background gas can be a limiting factor. Our experience

[1]This technique was common in the laboratory of W. Nagourney and H. Dehmelt at the University of Washington for deshelving Ba^+ ions in the long-lived $^2D_{3/2}$ and $^2D_{5/2}$ when one of us (J.R.T.) was a postdoc there. The plasma source was a commercial dc hollow-cathode lamp.

indicates that the background pressure must be less than 1×10^{-10} torr, although this limitation presumably depends upon the ion species and charge state under study and the composition of the background gas. In particular, as the charge state increases, charge exchange reactions become more likely, presumably placing stronger limitations on background gas pressure.

ACKNOWLEDGMENTS

This work was supported by the Laboratory Directed Research and Development program at Los Alamos National Laboratory, operated by Los Alamos National Security, LLC, for the NNSA US Department of Energy under Contract No. DE-AC52-06NA25396.

[1] V. A. Dzuba, V. V. Flambaum, and M. V. Marchenko, Phys. Rev. A **68**, 022506 (2003).

[2] V. A. Dzuba and V. V. Flambaum, Phys. Rev. A **77**, 012515 (2008).

[3] S. G. Porsev, V. V. Flambaum, and J. R. Torgerson, Phys. Rev. A **80**, 042503 (2009).

[4] M. Stobiska, G. Alber, and G. Leuchs, Europhys. Lett. **86**, 14007 (2009).

[5] C. Tamm, T. Schneider, and E. Peik, in *Astrophysics, Clocks and Fundamental Constants*, edited by S. Karshenboim and E. Peik (Springer, Berlin, 2004), p. 247.

[6] W. G. Rellergert, D. DeMille, R. R. Greco, M. P. Hehlen, J. R. Torgerson, and E. R. Hudson, Phys. Rev. Lett. **104**, 200802 (2010).

[7] C. J. Campbell, A. V. Steele, L. R. Churchill, M. V. DePalatis, D. E. Naylor, D. N. Matsukevich, A. Kuzmich, and M. S. Chapman, Phys. Rev. Lett. **102**, 233004 (2009).

[8] R. J. Jones, K. D. Moll, M. J. Thorpe, and J. Ye, Phys. Rev. Lett. **94**, 193201 (2005).

[9] C. Gohle, T. Udem, M. Herrmann, J. Rauschenberger, R. Holzwarth, H. A. Schuessler, F. Krausz, and T. W. Hansch, Nature (London) **436**, 234 (2005).

[10] S. Witte, R. T. Zinkstok, W. Ubachs, W. Hogervorst, and K. S. E. Eikema, Science **307**, 400 (2005).

[11] P. Ghosh, *Ion Traps* (Oxford University Press, Oxford, 1995).

[12] F. Vedel, Int. J. Mass Spectrom. Ion Proc. **106**, 33 (1991).

[13] R. Wuerker, H. Shelton, and R. Langmuir, J. Appl. Phys. **30**, 342 (1959).

[14] R. March, A. McMahon, F. Londry, R. Alfred, J. Todd, and F. Vedel, Int. J. Mass Spectrom. Ion Proc. **95**, 119 (1989).

[15] C. Balzer, A. Braun, T. Hannemann, C. Paape, M. Ettler, W. Neuhauser, and C. Wunderlich, Phys. Rev. A **73**, 041407(R) (2006).

[16] A. H. Nizamani, J. J. McLoughlin, and W. K. Hensinger, Phys. Rev. A **82**, 043408 (2010).

[17] D. Das, S. Barthwal, A. Banerjee, and V. Natarajan, Phys. Rev. A **72**, 032506 (2005).

[18] B. Fawcett and M. Wilson, At. Data Nucl. Data Tables **47**, 241 (1991).

[19] F. Vedel and J. Andre, Phys. Rev. A **29**, 2098 (1984).

[20] L. Hornekaer, N. Kjaergaard, A. M. Thommesen, and M. Drewsen, Phys. Rev. Lett. **86**, 1994 (2001).

[21] D. J. Seidel and L. Malecki, Phys. Rev. A **51**, R2699 (1995).

[22] K. Sugiyama and J. Yoda, Phys. Rev. A **55**, R10 (1997).

[23] Z. Zhang, Z. Li, S. Svanberg, P. Palmeri, P. Quinet, and E. Biemont, Eur. Phys. J. D **15**, 301 (2001).

[24] J. R. Torgerson (private communication).